17th Australasian Fluid Mechanics Conference
Auckland, New Zealand
5-9 December 2010

A Numerical Study on the Physiological Pulsatile Flow through an Eccentric Arterial Stenosis

A.B.M. Toufique Hasan[1], Sumon Saha[2], Md. Tarekul Alam[3], Md. Nasim Hasan[1], Md. Arif Hasan Mamun[1] and A.K.M. Sadrul Islam[4]

[1]Department of Mechanical Engineering
Bangladesh University of Engineering and Technology (BUET), Dhaka 1000, Bangladesh

[2]Department of Mechanical Engineering
University of Melbourne, Victoria 3010, Australia

[3]Department of Mechanical and Nuclear Engineering
Pennsylvania State University, University Park, PA 16802, USA

[4]Department of Civil and Environmental Engineering
Islamic University of Technology (IUT), Board Bazar, Gazipur 1704, Bangladesh

Abstract

In the present study, a numerical simulation is carried out to investigate the physiological pulsatile blood flow through an arterial stenosis. A semicircular eccentric stenosis is considered which is more relevant in cardiovascular system rather than the symmetric one. The degree of stenosis is varied by area from 30% to 70%. The pulsatile flow is represented by eight harmonic components superimposed on the time-mean flow. The Reynolds number is varied from 220 to 800 during the pulsation while the Womersley number was kept fixed at 6.17. Results show that the flow behaviours significantly vary during the pulse period. Moreover, vortex rings are developed asymmetrically and the post stenotic areas are severely affected by the vortex rings at the end of the systolic phase compared to other times. This disturbance is increased with an increase of degree of stenosis.

Introduction

Cardiovascular disease is one of the main causes of health risks in many countries and the atherosclerosis is the leading disease in the human cardiovascular system. This disease is formed by the hardening of arteries due to the deposition of plaque by the fatty substances in the blood. This constricts the blood flow passage area. Thus impose additional load on the heart and can lead to a stroke or a heart attack.

The fluid dynamical behaviour of blood flow through constricted channel has been studied for the last many years. Ahmed and Giddens [1], Ohja et al. [11] experimentally visualized the post stenotic behaviour of pulsatile flow through stenoses. Beyond these, there are many computational researches on the investigation of pulsatile flow in stenotic geometries [2, 4, 6, 8, 10, 12, 13]. Further, review on the modeling studies and experiments on steady and unsteady, two and three dimensional flows in arterial geometries most relevant in the context of atherosclerosis can be found in [3, 7]. However, most of the previous researches were based on the assumption of symmetric stenoses in the artery. In addition, these researches considered the simple pulsatile flow. In the present study, a numerical simulation has been carried out to investigate the physiological pulsatile flow through an eccentric arterial stenosis which is more relevant in cardiovascular system. A semicircular eccentric stenosis is considered with degree of stenosis varying from 30% to 70% by area. Various fluid dynamical characteristics for the flow through an arterial stenosis such as vortex dynamics, wall shear stress and so on are discussed during the pulse period.

Governing Equations and Numerical Method

Although the blood is known to be non-Newtonian in general, in the present study, it is assumed to be Newtonian, homogeneous, and incompressible. This is because it is considered large arteries with radii of the order of 1.0 mm, where the velocity and shear rate are high. The apparent viscosity is nearly a constant in arteries with relatively large diameters (~ 5mm), and therefore the non-Newtonian effects can be neglected [5]. The governing equations are the 2D Navier-Stokes equations of motion and mass continuity. Further, since in the present study, the Reynolds number is below 1000, the flow can be modeled by laminar modeling which is equivalent to turbulence modeling [10].

The governing equations are discretized by the weak formulation of finite element method (FEM). The computational domain is subdivided into finite number of elements. The elements used are the isoparametric triangular and the discretization is shown in Fig. 1(a). Quadratic and linear interpolation functions are used for velocity and pressure, respectively. For time integration, second order accurate implicit backward difference formulation is used.

Model artery and Computational Conditions

A simple model of a planar artery with one-sided semicircular stenosis is considered in the present study as shown in Fig. 1(a). The height of the artery H is 8mm. The degree of stenosis is defined as, $s = (H-h)/H \times 100\%$. The domain extends to $8H$ and $24H$ upstream (L_u) and downstream (L_d) from the center of the stenosis, respectively. The total number of degrees of freedom in each element is 15 and the computational domain is discretized with about 25000 such elements which show the grid independent solution. The viscosity of the blood μ is taken as 3.5×10^{-3} Pa.s with a mass density ρ of 1060 kg/m^3. The volumetric flow waveform in the common carotid artery of a healthy adult is considered in the present study as shown in figure 1(b) [8]. The heart rate is taken as 75bpm (pulse period, t_p= 0.8s) and the corresponding Womersley parameter ($\alpha = H/2\sqrt{2\pi\rho/t_p\mu}$) becomes 6.17. It is featured by a maximum acceleration in systolic phase (point a, t/tp = 0.15), main peak with zero acceleration in systole (point b, t/tp = 0.2), maximum deceleration in systole (point c, t/tp = 0.24), second peak in systole (point d, t/tp = 0.32), end of systole (point e, t/tp = 0.52) and main peak in the diastolic phase (point f, t/tp = 0.58). The mean Reynolds number, $Re = \frac{\rho Q}{\mu}$ is 345 with maximum and

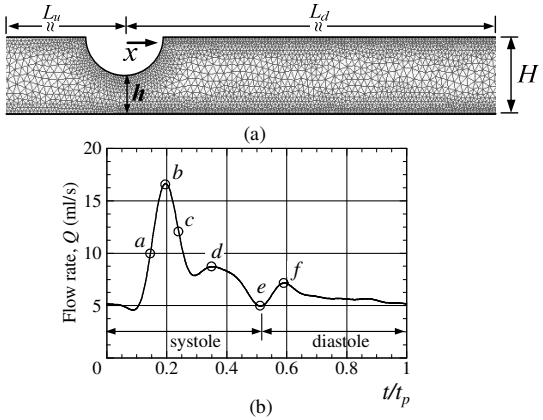

Figure 1. (a) Schematic of an eccentric arterial stenosis of 50% degree and (b) physiological flow waveform through an adult carotid artery [8]

minimum values being 800 and 220, respectively. Since the Womersley number of interest here is much greater than one, the inflow
velocity profile for fully developed periodic pulsatile laminar flow is different from that of parabolic shape and can be obtained in an analytic closed form [9, 14], which is the sum of Fourier-Bessel components at each temporal harmonic n defined by

$$u_n(y,t) = -i\,\frac{A_n}{\rho}\,\frac{t_p}{2\pi}\left(1-\frac{J_0(i^{3/2}\alpha\, y/H)}{J_0(i^{3/2}\alpha)}\right)\exp(i2n\pi t/t_p) \qquad (1)$$

where $i = (-1)^{1/2}$, J_0 ( ) is the complex Bessel function of order zero. The parameter A_n is the complex number representing the driving pressure gradient $\partial_x p = A_n \exp(i2n\pi t/t_p)$. In the present study the value of n is considered to be 8 which results approximately the same physiologically realistic flow waveform shown in figure 1(b) [8]. The resultant harmonic components can then be added on to the mean steady component to get the physiological flow waveform.

All the arterial walls are considered to be no-slip. At the outlet, a convective boundary condition is applied and this allows the vortex structures to exit the domain with minimal reflections.

Results and Discussion

Results obtained using the present computations are compared with the previous experimental results of Ojha et al. [10] for the validation of numerical simulation. The geometry was an axisymmetric 45% stenosis (by area) with a trapezoidal profile and the pulsatile flow had a sinusoidal waveform of 4.3±2.6 ml with a period of 345 ms. Experimental and computed centerline velocity variations with time at inlet and at different post stenotic regions are shown in figues 2(a) and (b), respectively. From these figures it can be concluded that the present computation can predict the arterial stenosis flow with reasonable accuracy. However, some discrepancies are observed near the peaks of the pulsatile flow.

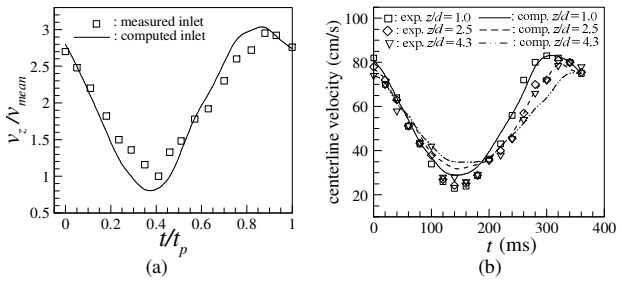

Figure 2. Comparison of the present numerical computation with that carried out by Ojha et al. [11]; (a) inlet centerline velocity profile and (b) centerline axial velocity at different post stenotic region

Figure 3 shows the instantaneous streamlines of the flow through an eccentric arterial stenosis at six stages of the pulse (as indicated in figure 1(b)) for different degrees of stenosis. At phase a (figure 3(a)) where the flow has maximum acceleration, fast increase in velocity results in the development of a vortex near upper wall just downstream of the stenosis. The vortices are merely in elliptic shape and vortex centers are at $x/H \approx 0.5$, 0.8 and 1.4 for 30%, 50% and 70% degree of stenosis, respectively. The corresponding lengths of the major axes are about 0.3H, 0.7H and 1.3H. However, shear layers are generated from the lip of the stenosis which are more pronounced at 50% and 70% stenosis. Lift of streamlines from the lower wall is observed for 70% stenosis. At the phase b of maximum flow rate (figure 3(b)), reduction of flow acceleration causes the vortices to break into two pieces of previously formed vortices around the upper wall. Furthermore, the separated shear layer reattaches to the upper wall at $x/H \approx 2.2$ and 3.4 for 50% and 70% stenosis, respectively. This reattachment causes to form a vortex at the lower wall. The center of the lower wall vortex approximately corresponds to the reattachment point of the shear layer at upper wall. At next phase c of maximum deceleration at systole (figure 3(c)), three distinguish sized vortices are found around the stenosis upper

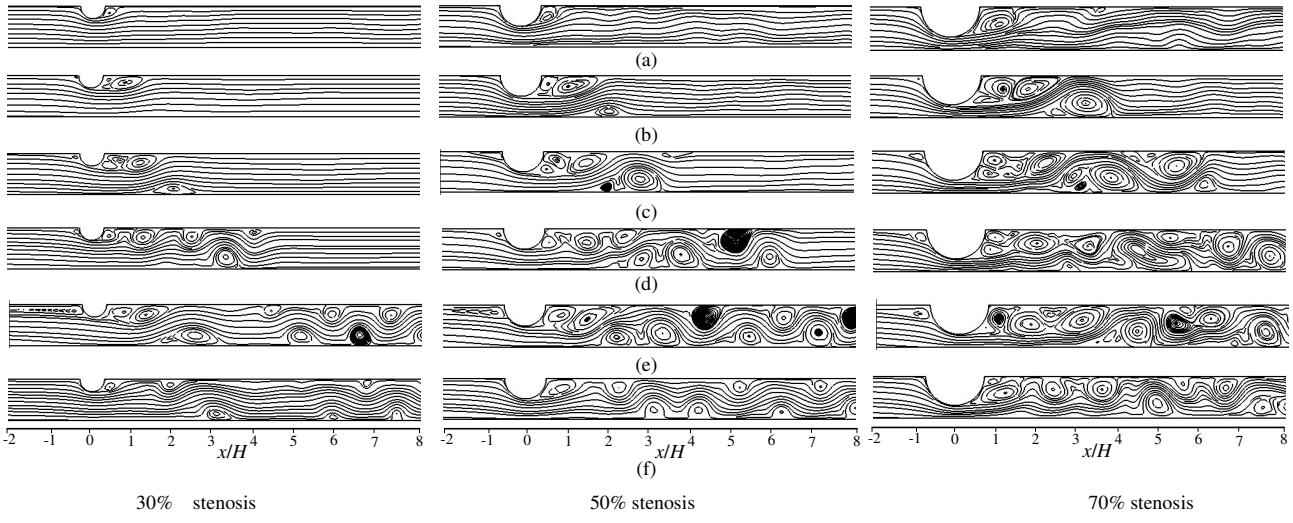

Figure 3. Instantaneous streamlines of the flow at six stages of the pulse across three eccentric stenosis of 30%, 50% and 70% degrees; (a) $t/t_p = 0.15$, (b) $t/t_p = 0.20$, (c) $t/t_p = 0.24$, (d) $t/t_p = 0.32$, (e) $t/t_p = 0.52$ and (f) $t/t_p = 0.58$.

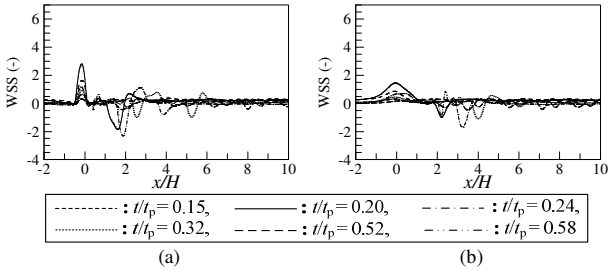

(a) (b)

Figure 4. Instantaneous wall shear stress for 50% eccentric stenosis; (a) upper wall and (b) lower wall

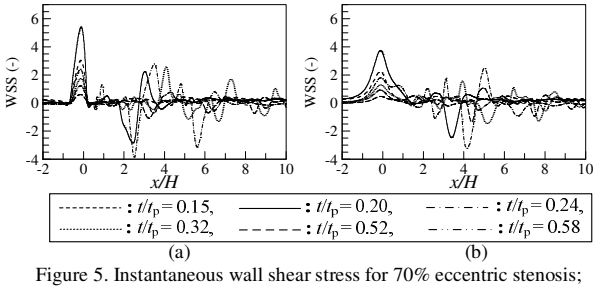

(a) (b)

Figure 5. Instantaneous wall shear stress for 70% eccentric stenosis; (a) upper wall and (b) lower wall

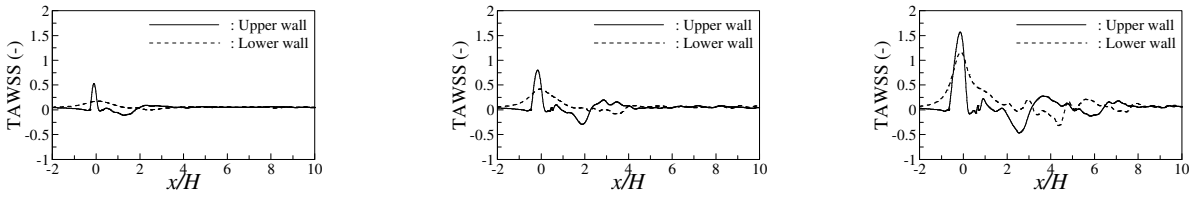

(a) (b) (c)

Figure 6. Time averaged wall shear stress (TAWSS) for different eccentric stenosis degrees; (a) 30%, (b) 50% and (c) 70%

wall area. Here, lower wall vortex can be seen for smallest stenosis of 30% as well. However, lower wall single vortex is broken into several pieces for 50% and 70% stenosis. Moreover, in these two stenoses, the separated shear layer reflects from the upper wall and further reattaches at lower wall. These cause to generate additional vortices at the upper wall whose centers are at $x/H \approx 4.0$ and 5.5 for 50% and 70% stenosis, respectively. Further, at second peak in systole (phase *d*), the vortices in the stenosed artery break up and convect downstream as a complex array of vortex structures shown in figure 3(d). In this case, vortex rings can be seen upto $x/H = 4.2$, 5.8 and 8.0 for 30%, 50% and 70% stenosis, respectively. However, at 70% stenosis, some vortices are stretched by the complex interaction of shear layer on vortices (at $x/H \approx 5.0$). At phase *e* (figure 3(e)), the vortices are growing in size and vortices are seen far downstream of the stenosis. In addition, at upstream of the stenosis, recirculation is observed at this time. At the diastole (phase *f,* figure 3(f)), vortices become smaller due to viscous dissipation and take the regular shape of a circle compared to the previous phases. It can be concluded that during the pulsation, vortices are generated asymmetrically in the stenosed artery and post stenotic regions are severely affected by the vortex rings at the end of the systolic phase.

It is recognized that the wall shear stress (WSS) is the primary fluid mechanical properties that affect the biological arterial response [7]. WSS is divided by fluid dynamic head, $1/2\rho(Q_{av}/H)^2$ and the non-dimensionalized form is shown in this section. Figure 4 shows the instantaneous WSS for 50% stenosis. It is found that the WSS is fluctuating during the cycle. WSS reaches the peak near the lip of the stenosis and further distribute downstream with positive and negative magnitudes which correspond to the counter rotating vortices in the stenosed artery. The positive peak WSS is found at $t/t_p = 0.2$ due to the maximum flow rate and the minimum occurs at $t/t_p = 0.52$ (end of systole). However, fluctuation in WSS is found upto $x/H \approx 6.0$ for upper wall (figure 4(a)). In case of lower wall (figure 4(b)), the peak WSS region is flatter and the magnitude is smaller to those in upper wall. In this case, the WSS fluctuation is seen upto $x/H \approx 4.5$. In addition, during cycle, the negative peak at $x/H \approx 3.0$ is in comparable manner to positive peak at $x/H = 0$. However, in upper wall the positive peak is 1.3 times higher that the negative peak of WSS.

Results for 70% stenosis are shown in figure 5. The main peak WSSes are about 1.9 times and 2.3 times higher than those of 50% stenosis for upper and lower walls, respectively. WSS fluctuates upto $x/H \approx 10.0$ and $x/H \approx 8.0$ for upper and lower walls, respectively. In upper wall (figure 5(a)) the positive peak is about 1.5 times higher that the negative peak of WSS. In case of lower wall (figure 5(b)), the peaks are in comparable manner.

The time averaged wall shear stress (TAWSS) is evaluated considering a cardiac cycle and the distribution is shown in figure 6. It is found that the TAWSS at upper wall is 3 times, 2 times and 1.3 times higher than the lower TAWSS for 30%, 50% and 70% stenosis, respectively. Thus with increasing the degree of stenosis, the lower wall TAWSS increased significantly. The significant TAWSS are observed along upper wall upto $x/H = 3.0$, 4.0 and 8.0 with multiple changes in signs for 30%, 50% and 70% stenosis, respectively. Further, significant region of negative TAWSS is found at lower wall for 50% and 70% stenoses. This means that the lower wall is also affected by the upper wall stenosis. With an increase of degree of stenosis, this effect becomes prominent.

The wall shear stress gradient (WSSG) is a parameter which indicates the changes in shearing forces, and hence 'aggravating effect' on the endothelium lining on the arterial wall [4]. The peak WSSG signifies the regions of flow acceleration and deceleration. Several peaks are observed in an eccentric stenosis as shown in figure 7. Peaks are distributed upstream and downstream of the stenosis. However, the number and the magnitudes of peaks are increased with an increase of degree of stenosis. Significant WSSG with fluctuating magnitudes along upper wall are found upto $x/H \approx 4.0$, 6.0 and 10.0 for 30%, 50% and 70% stenosis, respectively. Moreover, though WSSG along lower wall is zero in 30% stenosis, considerable WSSG can be observed further downstream of the stenosis for an artery with large stenosis. This is due to extended temporal interaction of vortices with lower wall in large stenosed artery.

The cyclic variation of WSS is often expressed in terms of the oscillatory shear index (OSI). OSI is defined as [4]:

$$\mathrm{OSI} = \frac{1}{2}\left(1 - \frac{\tau_{mean}}{\tau_{mag}}\right) \qquad (2)$$

where τ_{mean} represents the mean shear stress to express the magnitude of the time-averaged surface traction vector and τ_{mag} represents the time averaged magnitude of the wall shear stress vector. The OSI varies between 0 and 0.5 and the peak values indicate the points of time averaged separation and reattachment.

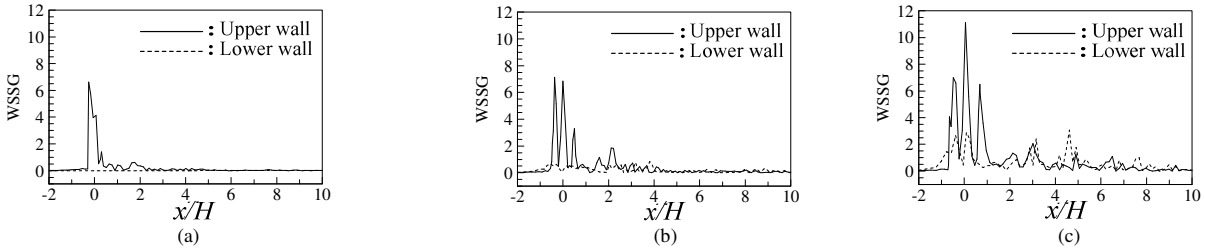

Figure 7. Wall shear stress gradient (WSSG) for different eccentric stenosis degrees; (a) 30%, (b) 50% and (c) 70%

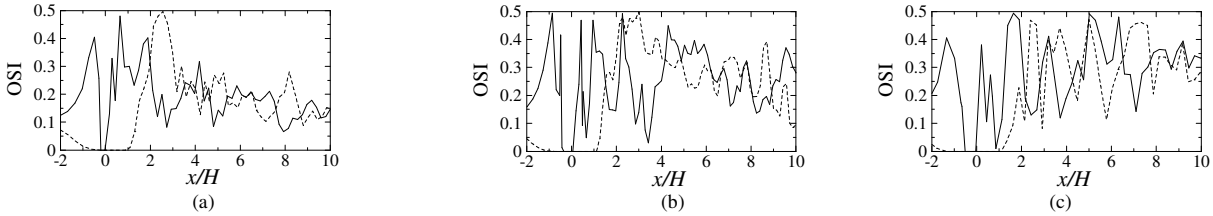

Figure 8. Oscillatory shear index (OSI) for different eccentric stenosis degrees; (a) 30%, (b) 50% and (c) 70%

Figure 8 shows the OSI distribution for different eccentric stenotic artery. OSI distribute apparently as the same manner as TAWSS (figure 6) and WSSG (figure 7). Thus, it can be concluded that the OSI distribute more unevenly and becomes oscillatory at the post stenotic regions with an increase of degree of stenosis both for upper and lower walls.

Conclusions

Physiological pulsatile blood flow through an eccentric arterial stenosis is studied numerically. The degree of stenosis is varied by area from 30% to 70%. The physiological flow is represented by eight harmonic components superimposed on the time-mean flow. The Reynolds number is varied from 220 to 800 during the pulsation while the Womersley number was kept fixed at 6.17. Results can be summarized as follows:

(1) Shear layers and vortex rings are generated asymmetrically in the stenosed artery and distribute in the post stenotic regions. This behaviour becomes more severe at the end of systolic phase.
(2) The hemodynamic parameter such as WSS fluctuates during the pulse period corresponding to the physiological flow. The fluctuating characteristics increase with an increase of degree of stenosis.
(3) Mean flow characteristics such as TAWSS shows that lower wall together with upper wall is also affected by the interaction of shear layer and the vortex and this effect becomes prominent in artery with large degree of stenosis.
(4) WSSG and OSI show that the reattachment and separation are distributed upstream and downstream of the stenosis. And the flow becomes more pulsatile in the post stenotic regions with increasing degree of stenosis both for upper and lower walls.

References

[1] Ahmed, S.A. & Giddenss, D.P., Pulsatile Poststenotic Flow Studies with Laser Doppler Anemometry, *J. Biomech*, **17**, 1984, 695-705.

[2] Beratlis, N., Balaras, E., Parvinian, B. & Kiger, K., A Numerical and Experimental Investigation of Transitional Pulsatile Flow in a Stenosed Channel, *J. Biomech. Engg.*, **127**, 2005, 1147-1157.

[3] Berger, S.A. & Jou, L.D., Flows in Stenotic Vessels, *Annu. Rev.Fluid Mech.*, **32**, 2000, 347-382.

[4] Buchanan, Kleinstreuer, Jr.C. & Comer, J.K., Rhelogical Effects on Pulsatile Hemodynamics in a Stenosed Tube, *Comp. Fluids*, **29**, 2000, 696-724.

[5] Fung, Y.C., *Biomechanics: Circularion*, New York: Springer-Verlag, 1997.

[6] Griffith, M.D., Leweke, T., Thompson, M.C. & Hourigan, K., Pulsatile Flow in Stenotic Geometries: Flow Behaviour and Stability, *J. Fluid Mech.*, **622**, 2009, 291-320.

[7] Ku, D.N., Blood Flow in Arteries, *Annu. Rev.Fluid Mech.*, **29**, 1997, 399-434.

[8] Long, Q., Xu, X.Y., Ramnarine, K.V. & Hoskins, P., Numerical Investigation of Physiologically Realistic Pulsatile Flow Through Arterial Stenosis, *J. Biomech*, **34**, 2001, 1229-1242.

[9] Nichols, W.W. & O'Rourke, M.F., *McDonald's Blood Flow in Arteries: Theoretical, Experimental and Clinical Principles*, Oxford University Press, 1998.

[10] Nosovitsky, V.A., Ilegbusi, O.J., Jiang, J., Stone, P.H. & Feldman, C.L., Effects of Curvature and Stenosis-like Narrowing on Wall Shear Stress in a Coronary Artery Model with Phasic Flow, *J. Comp. Biomed. Res.*, **30**, 1997, 61-82.

[11] Ohja, M., Cobbold, R.S.C., Johnston, K.W. & Hummel, R.L., Pulsatile Flow Through Constricted Tubes: an Experimental Investigation using Photochromic Tracer Method, *J. Fluid Mech.*, **203**, 1989, 173-197.

[12] Paul, M.C., Molla, M.M. & Roditi, G., Large-eddy Simulation of Pulsatile Blood Flow, *Med. Engg Physics*, **31**, 2009, 153-159.

[13] Varghese, S.S. & Frankel, S.H., Numerical Modeling of Pulsatile Turbulent Flow in Stenotic Vessels, *J. Biomech. Engg.*, **125**, 2003, 445-460.

[14] Womersley, J.R., Method for the Calculation of Velocity, Rate of Flow and Viscous Drag in Arteries when the Pressure Gradient is Known, *J. Physiol.*, **127**, 1955, 553-563.